# Effects of spin-dependent electronic correlations on surface states in topological insulators

Z. Toklikishvili,[1] L. Chotorlishvili,[2] S. Stagraczyński,[3] V. K. Dugaev,[3] A. Ernst,[4,5] J. Barnaś,[6,7] and J. Berakdar[2]

[1]*Faculty of Exact and Natural Sciences, Tbilisi State University, Chavchavadze Avenue 3, 0128 Tbilisi, Georgia*

[2]*Department of Physics, Martin-Luther-Universität Halle-Wittenberg, 06120 Halle, Germany*

[3]*Department of Physics and Medical Engineering, Rzeszów University of Technology, 35-959 Rzeszów, Poland*

[4]*Institute for Theroretical Physics, Johannes Kepler University, Altenberger Straße 69, 4040 Linz, Austria*

[5]*Max Planck Institute of Microstructure Physics, Weinberg 2, D-06120 Halle, Germany*

[6]*Faculty of Physics, Adam Mickiewicz University, ulica Uniwersytetu Poznańskiego 2, 61-614 Poznań, Poland*

[7]*Institute of Molecular Physics, Polish Academy of Sciences, ulica Mariana Smoluchowskiego 17, 60-179 Poznań, Poland*

(Received 19 August 2019; revised manuscript received 30 October 2019; published 11 December 2019)

The effect of electron-electron interactions on the energy spectrum of surface electrons in a three-dimensional topological insulator is studied theoretically. The interaction includes both charge- and spin-dependent correlations. Using the Green's function method, we calculate the electron self-energy and determine the renormalized spin-orbit coupling strength. We find that the energy spectrum renormalized by spin-dependent electronic correlation turns nonlinear with respect to the wave vector $k$ measured from the perfect Dirac cone (in the absence of electron-electron interactions). We also discuss charge screening contributions from surface and bulk electrons.

DOI: 10.1103/PhysRevB.100.235419

## I. INTRODUCTION

Topological insulators (TIs) form a class of materials with specific topological properties of electron energy bands [1,2]. It was predicted theoretically that a two-dimensional electron gas (2DEG) appears by necessity at the interface between topologically nonequivalent insulators—including the TI-vacuum interface as a particular case. TIs have surface electron states with relativistic-type (Dirac) gapless energy spectra, resulting in distinct physical features such as robustness to perturbations that preserve time-inversion symmetry. Owing to spin-momentum locking, a chiral spin mode appears at the surfaces of TIs, as observed experimentally [3].

Properties of TIs have been studied extensively in the context of various physical phenomena, such as the spin Hall effect, nonequilibrium topological states, antiferromagnetic magnonic spintronics, interfacial skyrmions on the surface of a TI, and Klein tunneling [4–15]. Recently, current-induced spin-orbit torques and magnetic switching in hybrid TI-ferromagnet heterostructures and in a TI with magnetic molecules on its surface were also analyzed [16–18]. Furthermore, features akin to TIs were exploited for the interconversion of spin and charge currents and for the generation of thermally assisted magnonic spin currents [19–21]. Because of the proximity effect, magnetic structures on the surface of TIs, like, for instance, magnetic impurities [22–24], magnetic stripes, or helicoidal magnetic structures [25], were also shown to have a substantial influence on the electronic band structure of the surface states of TIs and may even suppress the topological phase.

Most physical properties of TIs are derivable from a one-particle description of their electronic structure. The role of electronic and spin correlations is relatively less explored [20,26–41]. Generally, the electron-electron interaction leads to a renormalization and a finite lifetime of the energy states. The strength of the spin-orbit interaction can also be modified. Numerous first-principles studies demonstrated that a proper account of the electron-electron interaction, for instance, using the GW approximation [42], can correctly capture the spectral properties of both bulk and surface electronic states in TIs [43,44]. The impact of electron-electron interaction on the topological properties was found to be material specific. A strong nonlinearity of the topological states was found in $Bi_2Se_3$, while $Sb_2Te_3$ exhibits Dirac surface states with a linear dispersion [44]. At the same time, the electronic structures of $Bi_2Se_3$ and $Sb_2Te_3$ are almost unaffected by the screened Coulomb interaction [43]. It was also shown that neglecting the spin-orbit interaction leads only to a simple energy shift, while a proper accounting of all relativistic effects and screened Coulomb interaction results in a nontrivial dispersion of the topologically protected surface states, in good agreement with experiments [43,44]. The electron-electron interaction may also change the electron velocity or modify the anisotropy of the energy spectrum in the low-energy limit. Accounting for the vertex corrections in the GW approximation, it was also shown that plasma satellites may appear in the elementary excitation spectrum, which leads to a shift of the valence state bottom to a lower energy [45]. We note that similar effects have been already discovered in graphene [46–53].

The present contribution addresses the effect of spin-dependent electron-electron interaction on the energy spectrum of surface electrons in a three-dimensional (3D) topological insulator. Here, we calculate the electron self-energy while accounting for spin-independent (density-density) and spin-dependent (spin density-spin density) electron correlations. We analyze explicitly the impact of exchange and Hartree contributions to the self-energy and conclude that the

 

contributions of exchange diagrams lead to some deviation of the energy dispersion from the linear behavior. We also inspect correlation-induced corrections to the spin-orbit interaction and find the energy spectrum at $k \to 0$ is characterized by a higher electron velocity. Moreover, we analyze screening of the electron-electron interaction by surface and bulk electrons. While generally small, the latter contribution may turn comparable (or even larger) than the screening in two-dimensional (2D) electron systems.

In Sec. II, we present a theoretical model of a topological insulator with electron correlations. Self-energy due to electron-electron correlations (both Coulomb and spin-dependent) is calculated in Sec. III, showing that the exchange diagrams renormalize the band structure and give rise to some nonlinearity in the dispersion relations. In addition, electron-electron interactions modify the spin-orbit coupling strength. In Sec. IV, we show the result of using a self-consistent model for the electron energy spectrum of surface electrons. Charge screening is analyzed in Sec. V, where screening by both surface and bulk electrons is considered. Summary and final conclusions are in Sec. VI.

## II. THEORETICAL MODELLING

Two-dimensional surface electrons in TIs with electron-electron interaction included are described by the following Hamiltonian:

$$\begin{aligned} H = & -iv\,\psi^{\dagger}(\mathbf{r})\,(\sigma_x\nabla_y - \sigma_y\nabla_x)\,\psi(\mathbf{r}) \\ & + g_1(\mathbf{r}-\mathbf{r}')\,[\psi^{\dagger}(\mathbf{r})\,\psi(\mathbf{r})]\,[\psi^{\dagger}(\mathbf{r}')\,\psi(\mathbf{r}')] \\ & + g_2(\mathbf{r}-\mathbf{r}')\,[\psi^{\dagger}(\mathbf{r})\,\sigma_i\,\psi(\mathbf{r})]\,[\psi^{\dagger}(\mathbf{r}')\,\sigma_i\,\psi(\mathbf{r}')], \quad (1) \end{aligned}$$

where $\psi^{\dagger}(\mathbf{r})$ and $\psi(\mathbf{r})$ are spinor field operators, $\sigma_i$ $(i = x, y, z)$ are the spin Pauli matrices, and the functions $g_1(\mathbf{r}) = g_1(r)$ and $g_2(\mathbf{r}) = g_2(r)$ describe respectively the density-density and spin density–spin density interactions of electrons at a distance $r$.

The first term in Eq. (1) is the 2D Hamiltonian $H_0$ of free surface electrons in TIs without electron-electron interactions. The corresponding electron energy spectrum consists of two energy branches with a linear dispersion, $\varepsilon_{1,2}(k) = \pm vk$. Note that $v$ in our model depends on the strength of the bare spin-orbit interaction. Both $g_1(r)$ and $g_2(r)$ are screened and have the generic form in momentum $(q)$ space in 2D,

$$g_1(q) = \frac{2\pi e^2}{q+\kappa_1}, \qquad g_2(q) = \frac{2\pi e^2\lambda_0}{q+\kappa_2}, \quad (2)$$

where $\kappa_{1,2} > 0$ are the inverse screening lengths (with usually $\kappa_2 > \kappa_1$) and $\lambda_0$ stands for a dimensionless coupling parameter.

## III. SELF-ENERGY

The exchange and Hartree diagrams yield the following contributions to the self-energy of surface electrons:

$$\hat{\Sigma}_1^{\rm ex}(\mathbf{k}) = i\int \frac{d\varepsilon}{2\pi}\frac{d^2\mathbf{k}'}{(2\pi)^2}\, g_1(\mathbf{k}-\mathbf{k}')\,\hat{G}_0(\mathbf{k}',\varepsilon), \quad (3)$$

$$\hat{\Sigma}_2^{\rm ex}(\mathbf{k}) = i\int \frac{d\varepsilon}{2\pi}\frac{d^2\mathbf{k}'}{(2\pi)^2}\, g_2(\mathbf{k}-\mathbf{k}')\,\sigma_i\,\hat{G}_0(\mathbf{k}',\varepsilon)\,\sigma_i, \quad (4)$$

$$\hat{\Sigma}_1^{H}(\mathbf{k}) = -ig_1(0)\sigma_0\,{\rm Tr}\int \frac{d\varepsilon}{2\pi}\frac{d^2\mathbf{k}'}{(2\pi)^2}\,\hat{G}_0(\mathbf{k}',\varepsilon), \quad (5)$$

$$\hat{\Sigma}_2^{H}(\mathbf{k}) = -ig_2(0)\int \frac{d\varepsilon}{2\pi}\frac{d^2\mathbf{k}'}{(2\pi)^2}\,\hat{G}_0(\mathbf{k}',\varepsilon). \quad (6)$$

The subscript 1(2) refers to the Coulomb (spin-dependent) electron interactions, while $\sigma_0$ is the unit matrix in the spin space. The Green's function $\hat{G}_0(\mathbf{k})$ of free electrons at the surface of TI has the form

$$\hat{G}_0(\mathbf{k},\varepsilon) = \frac{\varepsilon+\mu+v\,\hat{\mathbf{z}}\cdot(\boldsymbol{\sigma}\times\mathbf{k})}{2vk}\left(\frac{1}{\varepsilon+\mu-vk+i\delta\,{\rm sgn}\,\varepsilon} - \frac{1}{\varepsilon+\mu+vk+i\delta\,{\rm sgn}\,\varepsilon}\right), \quad (7)$$

where $\mu$ is the chemical potential. Only when we deem it needed to avoid misunderstanding is $\sigma_0$ displayed; otherwise, it is suppressed.

Performing the integral over energy for the Green's function given by Eq. (7), one obtains

$$\int \frac{d\varepsilon}{2\pi}\,\hat{G}_0(\mathbf{k},\varepsilon) = \frac{i}{2}[\theta(\mu-vk) - \hat{\mathbf{z}}\cdot(\boldsymbol{\sigma}\times\mathbf{n}_{\mathbf{k}})\theta(vk-\mu)], \quad (8)$$

where $\mathbf{n}_{\mathbf{k}} = \mathbf{k}/k$. Substituting (2) and (8) into Eqs. (3)–(6), we find

$$\begin{aligned} \hat{\Sigma}_1^{\rm ex}(\mathbf{k}) = & -\frac{e^2}{2\pi}\int_0^{\pi} d\theta \int_0^{\mu/v} \frac{k'dk'}{\zeta(\mathbf{k},\mathbf{k}')+\kappa_1} \\ & + \frac{e^2\hat{\mathbf{z}}\cdot(\boldsymbol{\sigma}\times\mathbf{n}_{\mathbf{k}})}{2\pi}\int_0^{\pi} d\theta \int_{\mu/v}^{k_{\rm max}} \frac{k'dk'\cos\theta}{\zeta(\mathbf{k},\mathbf{k}')+\kappa_1}, \quad (9) \\ \hat{\Sigma}_2^{\rm ex}(\mathbf{k}) = & -\frac{3e^2\lambda_0}{2\pi}\int_0^{\pi} d\theta \int_0^{\mu/v} \frac{k'dk'}{\zeta(\mathbf{k},\mathbf{k}')+\kappa_2} \\ & - \frac{e^2\lambda_0\hat{\mathbf{z}}\cdot(\boldsymbol{\sigma}\times\mathbf{n}_{\mathbf{k}})}{2\pi}\int_0^{\pi} d\theta \int_{\mu/v}^{k_{\rm max}} \frac{k'dk'\cos\theta}{\zeta(\mathbf{k},\mathbf{k}')+\kappa_2}, \quad (10) \end{aligned}$$

$$\hat{\Sigma}_1^{H}(\mathbf{k}) = \frac{e^2\mu^2}{4v^2\kappa_1}, \quad (11)$$

$$\hat{\Sigma}_2^{H}(\mathbf{k}) = \frac{e^2\lambda_0\mu^2}{2v^2\kappa_2}, \quad (12)$$

where $\zeta(\mathbf{k},\mathbf{k}') = \sqrt{k^2+k'^2-2kk'\cos\theta}$ and $\theta$ is the angle between the vectors $\mathbf{k}$ and $\mathbf{k}'$. Note that the integrals (9) and (10) contain the terms in the form of spin-orbit interaction (second terms). Both of them are formally divergent at the upper limit. This divergence is, however, removed by the cutoff at $k = k_{\rm max}$. This is fully justified because the linear dispersion of surface electrons (in which we are interested and for which our model is valid) describes only the low-energy region. The total self energy is a sum of all four contributions (9)–(12). The real part of self-energy determines the correction to the electron energy spectrum due to the interactions.

The Hartree contributions to the self-energy, Eqs. (11) and (12), do not depend on $k$. Correspondingly, they do not affect the energy structure. Such contributions can be viewed as a renormalization of the chemical potential. Therefore, one can

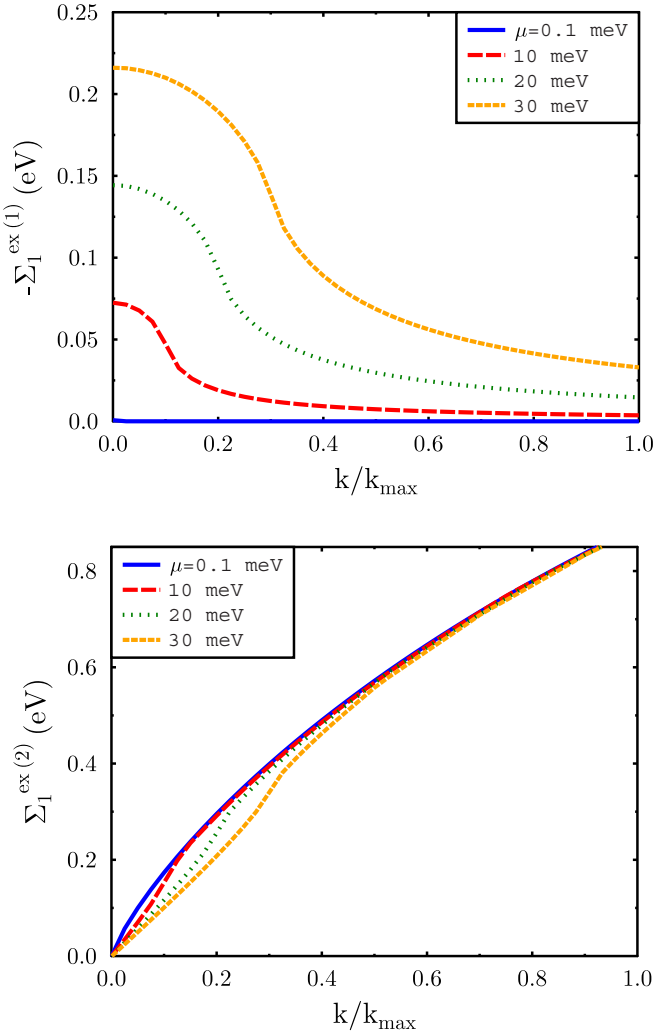


FIG. 1. Contributions $\Sigma_1^{ex(1)}$ and $\Sigma_1^{ex(2)}$, following from the charge density-density correlations, Eq. (9). Note that the corresponding full contribution to the self-energy is $\Sigma_1^{ex(1)} + \hat{\mathbf{z}} \cdot (\boldsymbol{\sigma} \times \mathbf{n_k}) \Sigma_1^{ex(2)}$. The dependence on wave vector $k$ is presented for different values of the chemical potential $\mu$. Other parameters as in the text.

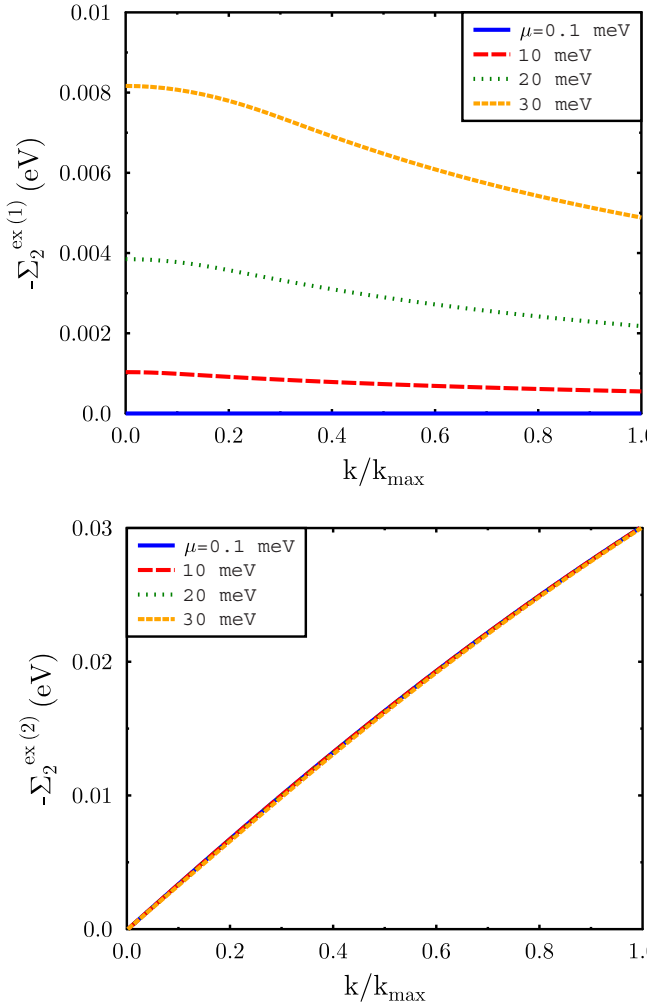


FIG. 2. Contributions $\Sigma_2^{ex(1)}$ and $\Sigma_2^{ex(2)}$, following from spin-dependent electron correlations to the first order in perturbation theory, Eq. (10). Full contribution to the self-energy is $\Sigma_2^{ex(1)} + \hat{\mathbf{z}} \cdot (\boldsymbol{\sigma} \times \mathbf{n_k}) \Sigma_2^{ex(2)}$. The dependence on wave vector $k$ is shown for different values of the chemical potential $\mu$. Other parameters as in the text.

exclude such terms assuming that the chemical potential is already properly renormalized.

For convenience, contributions from the exchange diagrams will be written as

$$\hat{\Sigma}_1^{ex}(\mathbf{k}) = \hat{\Sigma}_1^{ex(1)}(\mathbf{k}) + \hat{\mathbf{z}} \cdot (\boldsymbol{\sigma} \times \mathbf{n_k})\, \hat{\Sigma}_1^{ex(2)}(\mathbf{k}), \qquad (13)$$

where the first and second terms stand for the corresponding terms on the right-hand side of Eq. (9). Similar notation is also introduced for $\hat{\Sigma}_2^{ex}(\mathbf{k})$. The results of numerical calculations of $\hat{\Sigma}_1^{ex(1)}(\mathbf{k})$ and $\hat{\Sigma}_1^{ex(2)}(\mathbf{k})$ are shown in Fig. 1. In turn, results of similar calculations for $\hat{\Sigma}_2^{ex(1)}(\mathbf{k})$ and $\hat{\Sigma}_2^{ex(2)}(\mathbf{k})$ are shown in Fig. 2. In these calculations, we assumed the following parameters: $v = 10^{-8}$ eV cm, $\lambda_0 = 0.1$, $vk_{max} = 0.5$ eV, $\kappa_1 = 10^5$ cm$^{-1}$, and $\kappa_2 = 10^7$ cm$^{-1}$. Two terms $\Sigma_1^{ex(2)}$ and $\Sigma_2^{ex(2)}$ are responsible for the renormalization of the spin-orbit interaction. As we can see from Figs. 1 and 2, the contribution of the charge density-density interaction is much larger than that due to spin-dependent screening part, and it determines the nonlinear $k$ dependence of the renormalized spin-orbit coupling.

Using the self-energy $\Sigma(\mathbf{k})$, one can define the renormalized one-particle Hamiltonian as $\tilde{H}_0(\mathbf{k}) = H_0(\mathbf{k}) + \Sigma(\mathbf{k})$, which describes the renormalized energy spectrum of surface electrons. The corresponding energy spectrum is presented in Fig. 3, which reveals some nonlinearity in the dependence on the wave vector $k$. We note that this nonlinearity is an effect of electron-electron interaction to first order in the many-body perturbation theory.

## IV. SELF-CONSISTENT APPROACH

The results presented in Sec. III have been obtained in the first-order perturbation theory, and thus any higher order correction to the spectrum should be small. However, to get more realistic results one should sum up the higher order terms. Instead of this, we use a different (nonperturbative)

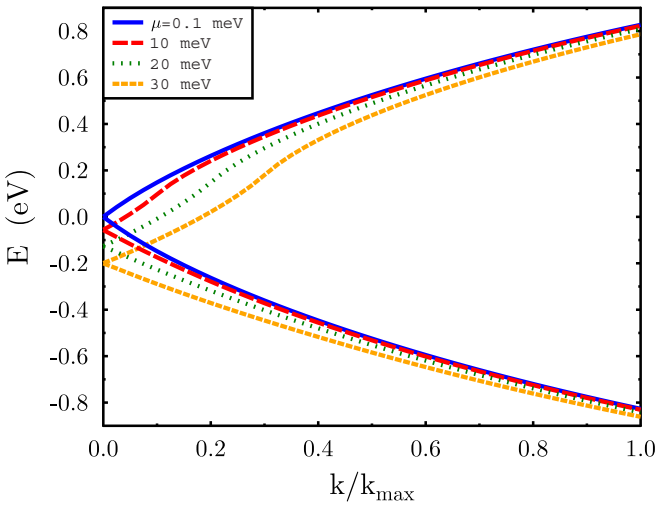


FIG. 3. Electron energy spectrum $E(k)$ with the contributions of $\Sigma_1^{\rm ex}$ and $\Sigma_2^{\rm ex}$ included. The dependence on wave vector $k$ is shown for different values of the chemical potential $\mu$. Other parameters are as in the text.

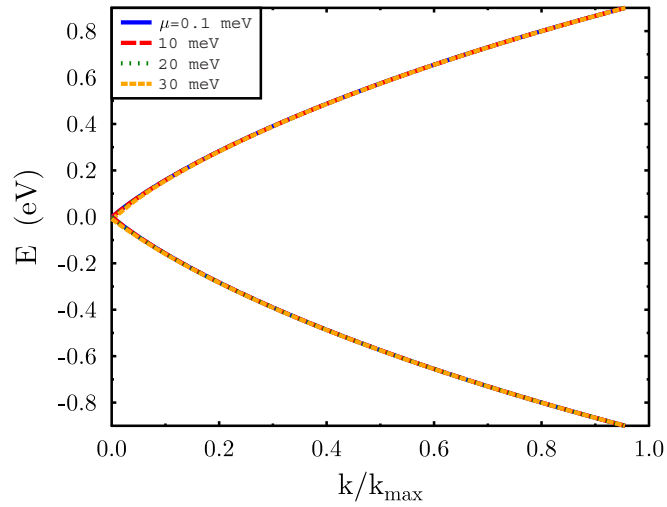


FIG. 4. The same as in Fig. 3 calculated by using the self-consistent model. After several iterations, there is no dependence on the location of chemical potential $\mu$.

approach, in which the electron-electron interaction is taken into account in a self-consistent way.

To do this, we present Hamiltonian of the system in the form

$$H = f_1(k) + v(\mathbf{k}\cdot\boldsymbol{\sigma})f_2(k), \tag{14}$$

where $f_{1,2}(k)$ are some unknown functions to be determined self-consistently. In the first-order perturbation theory, we found $f_1(k) = \Sigma_1^{\rm ex(1)} + \Sigma_2^{\rm ex(1)}$ and $f_2(k) = 1 + [\Sigma_1^{\rm ex(2)} + \Sigma_2^{\rm ex(2)}]/vk$. In agreement with the perturbation approach, one may assume that $f_1(k)$ is small and $f_2(k)$ is close to 1. As in the perturbation approach, the Hartree terms lead to a shift of the Fermi level, so we focus on the exchange terms only.

In the framework of self-consistent approach, we need to calculate the Green's function at a given step with the self-energies calculated in one step earlier. Accordingly, the self-energy should be calculated with full Green's function $\hat{G}(\mathbf{k},\varepsilon)$, which takes into account nonlinearity of the energy spectrum as described by Hamiltonian (14). Thus, we get

$$\hat{G}(\mathbf{k},\varepsilon) = \frac{\varepsilon - f_1(k) + \mu + v\hat{\mathbf{z}}\cdot(\boldsymbol{\sigma}\times\mathbf{k})f_2(k)}{2vk|f_2(k)|} \times\left(\frac{1}{\varepsilon-\varepsilon_1(k)+\mu+i\delta\,\mathrm{sgn}\,\varepsilon} - \frac{1}{\varepsilon-\varepsilon_2(k)+\mu+i\delta\,\mathrm{sgn}\,\varepsilon}\right), \tag{15}$$

where $\varepsilon_{1,2}(k) = f_1(k) \pm vk|f_2(k)|$ corresponds to the energy spectrum of the two bands.

Integration over $\varepsilon$ gives

$$\begin{aligned}\int\frac{d\varepsilon}{2\pi}\hat{G}(\mathbf{k},\varepsilon) = &-\frac{i}{4}\{\theta[\varepsilon_1(k)-\mu]-\theta[\mu-\varepsilon_1(k)]\\ &+\theta[\varepsilon_2(k)-\mu]-\theta[\mu-\varepsilon_2(k)]\}\\ &+\frac{i\hat{\mathbf{z}}\cdot(\boldsymbol{\sigma}\times\mathbf{n}_{\mathbf{k}})}{4}\{\theta[(\varepsilon_1(k)-\mu]-\theta[\mu-\varepsilon_1(k)]\\ &-\theta[\varepsilon_2(k)-\mu]+\theta[\mu-\varepsilon_2(k)]\},\end{aligned} \tag{16}$$

where we assumed $f_2(k) > 0$ since this function should be close to 1.

Let us assume $\varepsilon_2(k) < 0$ and $\mu > 0$. Then, $\theta[\varepsilon_2(k)-\mu] = 0$ , $\theta[\mu-\varepsilon_2(k)] = 1$, and we obtain

$$\int\frac{d\varepsilon}{2\pi}\hat{G}(\mathbf{k},\varepsilon) = \frac{i}{2}\theta[\mu-\varepsilon_1(k)] - \frac{i\hat{\mathbf{z}}\cdot(\boldsymbol{\sigma}\times\mathbf{n}_{\mathbf{k}})}{2} \times\theta[\varepsilon_1(k)-\mu]. \tag{17}$$

Thus, the only difference with Eq. (8) is that in the expression for $\Sigma^{\rm ex}(\mathbf{k})$ we have to substitute $\mu/v \to k_F$ in the limits of integration, where the Fermi wave vector $k_F$ is the solution of equation

$$f_1(k) + vkf_2(k) = \mu. \tag{18}$$

Using Eqs. (17) and (18) and Eqs. (9) and (10) with the substitution $\mu/v \to k_F$, we calculated the self-energy and electron energy spectrum by iterations starting from $f_1(k) = 0$ and $f_2(k) = 1$, which correspond to $\Sigma^{\rm ex}(\mathbf{k}) = 0$ (without electron-electron interactions). The self-consistent result is shown in Fig. 4. Thus, in the self-consistent approach the energy spectrum is nonlinear, and it does not depend on the chemical potential $\mu$ (compare Figs. 3 and 4).

## V. CHARGE SCREENING

Now we consider charge screening at the surface of TI. In general, one can distinguish two contributions to the screening: One of them is related to free electrons at the surface, and the other is due to electrons in the bulk of topological insulator.

### A. Screening by surface electrons

The polarization operator determining the renormalization of Coulomb interaction reads

$$\Pi(\mathbf{q},\omega) = -i\,\mathrm{Tr}\int\frac{d\varepsilon}{2\pi}\frac{d^2\mathbf{k}}{(2\pi)^2}G_0(\mathbf{k}+\mathbf{q},\varepsilon+\omega)G_0(\mathbf{k},\varepsilon). \tag{19}$$

Substituting the Green's function of surface electrons, Eq. (7), into Eq. (13), we find the following expression for the polarization operator at $\omega = 0$:

$$\Pi(\mathbf{q}, 0) = \int \frac{d^2\mathbf{k}}{(2\pi)^2}\left[\frac{f(\varepsilon_{\mathbf{k}+\mathbf{q}}) - f(\varepsilon_{\mathbf{k}})}{\varepsilon_{\mathbf{k}+\mathbf{q}} - \varepsilon_{\mathbf{k}}} + \frac{f(-\varepsilon_{\mathbf{k}+\mathbf{q}}) - f(-\varepsilon_{\mathbf{k}})}{\varepsilon_{\mathbf{k}} - \varepsilon_{\mathbf{k}+\mathbf{q}}}\right], \tag{20}$$

where $f(\varepsilon)$ is the Fermi-Dirac distribution function. The two terms in the above equation are related to the contributions of the two bands $\varepsilon_1(\mathbf{k}) \equiv \varepsilon_{\mathbf{k}} = vk$ and $\varepsilon_2(\mathbf{k}) = -\varepsilon_{\mathbf{k}}$.

In the limit of $q \to 0$, one obtains from Eq. (20)

$$\Pi(0, 0) = \frac{1}{2\pi}\int kdk[f'(\varepsilon_{\mathbf{k}}) + f'(-\varepsilon_{\mathbf{k}})]. \tag{21}$$

In particular, for $\varepsilon_{\mathbf{k}} = vk$, assuming the chemical potential $\mu > 0$, one finds $\Pi(0, 0) = -\mu/2\pi v^2$ at $T = 0$.

In the framework of the self-consistent approach, we have to use Green's functions (15) instead of $G_0(\mathbf{k}, \varepsilon)$ in Eq. (19). Then, using the energy spectrum $\varepsilon_{1,2}(k) = f_1(k) \pm vkf_2(k)$, we find

$$\Pi(0, 0) = -\frac{k_F}{2\pi\varepsilon_1'(k_F)}. \tag{22}$$

The Fourier transform of the renormalized electron interaction at the surface is

$$g(q) = \frac{g_0(q)}{1 - g_0(q)\,\Pi(q, 0)}, \tag{23}$$

where $g_0(q) = 2\pi e^2/q$ corresponds to the unscreened 2D Coulomb interaction in vacuum. In the limit of small $q$, we obtain

$$g(q) \simeq \frac{2\pi e^2}{q + \kappa_{1a}}, \tag{24}$$

where

$$\kappa_{1a} = -2\pi e^2\,\Pi(0, 0) \tag{25}$$

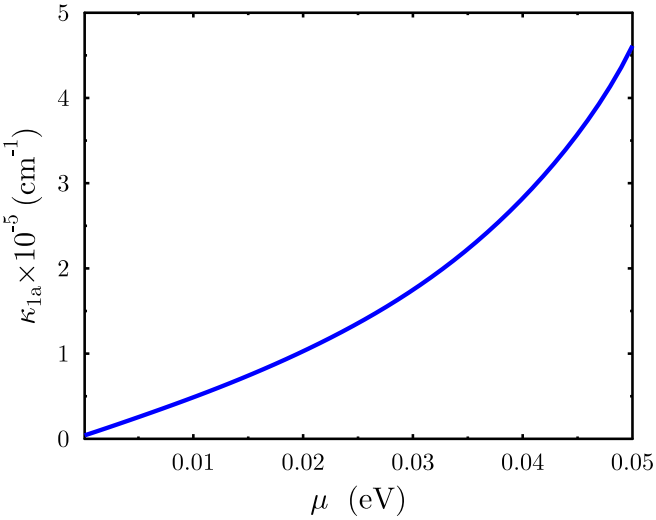


FIG. 5. Parameter $\kappa_{1a}$ calculated self-consistently and shown as a function of the chemical potential for the parameters described in the text.

is the inverse screening length related to the charge screening by 2D electrons at the surface of TI.

The dependence of parameter $\kappa_{1a}$ on chemical potential, calculated with polarization operator (22), is presented in Fig. 5. This dependence is a nonlinear function of $\mu$ due to nonlinearity of the electron energy spectrum (see Fig. 4).

### B. Screening by electrons in the bulk

To calculate the contribution to screening from bulk electrons, we start from the relation

$$g_{\mathbf{q}}(z, z') = g_{0,\mathbf{q}}(z, z') + \int_{-\infty}^{0} dz_1\, dz_2\; g_{0,\mathbf{q}}(z, z_1) \times \Pi_{\mathbf{q}}(z_1, z_2)\; g_{\mathbf{q}}(z_2, z'), \tag{26}$$

where $g_{0,\mathbf{q}}$ refers to the unscreened bare (Coulomb) interaction, and the polarization operator $\Pi_{\mathbf{q}}(z, z')$ at frequency $\omega = 0$ has to be calculated with the Green's functions of electrons in the bulk. In this equation, we used Fourier transformation in the $x$-$y$ surface plane

$$g_{\mathbf{q}}(z, z') = \int d^2\mathbf{r}\; g(\mathbf{r} - \mathbf{r}'; z, z')\; e^{-i\mathbf{q}\cdot(\mathbf{r}-\mathbf{r}')}. \tag{27}$$

The electronic structure in the bulk corresponds to the insulating state with the chemical potential in the gap. In the following, we omit the in-plane label $\mathbf{q} = (q_x, q_y)$.

We take into account that $g_0(z, z') = g_0(z - z')$ and $\Pi(z, z') = \Pi(z - z')$. Then Eq. (26) can be transformed to

$$g(z, z') = g_0(z - z') + \int_{-\infty}^{0} dz_1\, \chi(z - z_1)\, g(z_1, z'), \tag{28}$$

where

$$\chi(z) = \int \frac{dq_z}{2\pi}\,\Pi(q_z)\, g_0(q_z)\, e^{iq_z z}, \tag{29}$$

whereas $\Pi(q_z)$ and $g_0(q_z)$ are the Fourier transforms of the functions $\Pi(z - z')$ and $g_0(z - z')$, respectively.

With $z' = 0$ and denoting $g(z, 0) = W(z)$, one can write the following integral equation for the function $W(z)$:

$$W(z) = g_0(z) + \int_{-\infty}^{0} dz_1\, \chi(z - z_1)\, W(z_1), \tag{30}$$

with the asymptotic behavior

$$W(z) \sim e^{-qz},\; z \to \infty,$$
$$W(z) \sim e^{\kappa z},\; z \to -\infty. \tag{31}$$

Here, $\kappa$ is the inverse screening length in the bulk, which is assumed to be known. Our objective is to determine the inverse screening length $\kappa_{1b}$ of surface charges by bulk electrons, by relating $\kappa_{1b}$ to $\kappa$ in the bulk.

Equation (30) can be solved with the Wiener-Hopf method (see Appendix A). As a result, we obtain the following solution:

$$W(z) = \frac{2\pi e^2}{\sqrt{\kappa^2 + q^2}}\begin{cases} e^{-qz}, & z > 0, \\ e^{z\sqrt{\kappa^2+q^2}}, & z < 0. \end{cases} \tag{32}$$

Taking $z = 0$, one finds

$$W(0) \equiv g(0,0) = \frac{2\pi e^2}{\sqrt{\kappa^2 + q^2}}. \tag{33}$$

Correspondingly, a potential of a charge $e$ at the point $(0, 0, 0)$ is screened. At the point $(x, y, 0)$, it reads

$$g(r) = 2\pi e^2 \int \frac{d^2\mathbf{q}}{(2\pi)^2} \frac{e^{i\mathbf{q}\cdot\mathbf{r}}}{\sqrt{\kappa^2 + q^2}}. \tag{34}$$

Calculation of this integral at large distances, $\kappa r \gg 1$, leads to the interaction $g(r) = e^2 e^{-\kappa r}/r$ (see Appendix B). This behavior is mostly determined by the Fourier transform (33) at small $q \ll \kappa$. The Fourier transform (2) also leads to the same function $g(r)$ at large $r$. Therefore, one can approximately use the same form (2) for both types of screening, leading to the same asymptotics of interaction. Thus, we account for the screening of electron-electron interaction by surface and bulk electrons using $g_1(q)$ in Eq. (2) with $\kappa_1 = \kappa_{1a} + \kappa_{1b}$, where $\kappa_{1a}$ is determined by (18) and $\kappa_{1b}$ is the inverse screening length of the bulk, $\kappa_{1b} = \kappa$.

## VI. SUMMARY AND CONCLUSIONS

We have presented a theoretical description of the influence of electron-electron interactions on the surface states in topological insulators, taking into account the charge density-density and spin density-density interactions to first order in perturbation theory (Hartree and exchange contributions). By calculating the self-energy, we have found that the electron-electron interactions lead to some modification of the band structure. The exchange diagrams give rise to a nonlinearity of the electron dispersion relation. In the self-consistent approach, the spectrum is nonlinear and independent of the chemical potential (up to a shift due to Hartree terms). The electron-electron interactions also renormalize and enhance the spin-orbit coupling strength. The renormalized band structure may be observed directly in ARPES (angle-resolved photoemission spectroscopy) measurements. Furthermore, the renormalization of band structure may also have an impact on transport properties, especially on electron mobility at the Fermi level, which is important for high-frequency applications.

Screening of electric charges at the surface of TI was taken into account, and the contributions to the screening due to surface and bulk electrons were calculated. In the latter case, the corresponding inverse screening length has been related to the bulk screening length, and we have shown that at large distances it is equal to the bulk screening length.

## ACKNOWLEDGMENTS

This work was supported by the National Science Center in Poland as a research project, No. DEC-2017/27/B/ST3/02881. A.E. acknowledges financial support from DFG through priority program SPP1666 (Topological Insulators), SFB-TRR227, and OeAD Grants No. HR 07/2018 and No. PL 03/2018.

## APPENDIX A: SOLUTION OF EQ. (30) BY THE WIENER-HOPF METHOD

Following the Wiener-Hopf method we consider the extension of Fourier transform of $W(z)$,

$$W(k) = \int_{-\infty}^{\infty} dz\, W(z)\, e^{-ikz}, \tag{A1}$$

to complex $k$. In correspondence with (31),

$$W(z)\, e^{-ikz} \sim e^{-z(q - \mathrm{Im}\, k)}\, e^{-iz\, \mathrm{Re}\, k} \quad \text{as } z \to \infty, \tag{A2}$$

$$W(z)\, e^{-ikz} \sim e^{z(\kappa + \mathrm{Im}\, k)}\, e^{-iz\, \mathrm{Re}\, k} \quad \text{as } z \to -\infty. \tag{A3}$$

This means that for $z \to \infty$, the function $W(z)\, e^{-ikz} \to 0$, if $\mathrm{Im}\, k < q$, whereas for $z \to -\infty$ the function $W(z)\, e^{-ikz} \to 0$, if $\mathrm{Im}\, k > -\kappa$. Hence, the Fourier transform (A1) for complex $k$ is an analytic function of $k$ in the strip $-\kappa < \mathrm{Im}\, k < q$.

We present the function $W(z)$ as a sum [54,55]:

$$W(z) = W(z)\, \theta(z) + W(z)\, \theta(-z). \tag{A4}$$

Correspondingly, for the Fourier transform of $W(z)$, we get

$$W(k) = \varphi^+(k) + \varphi^-(k), \tag{A5}$$

where

$$\varphi^+(k) = \int_{-\infty}^{0} dz\, W(z)\, e^{-ikz}, \tag{A6}$$

$$\varphi^-(k) = \int_{0}^{\infty} dz\, W(z)\, e^{-ikz}. \tag{A7}$$

As one can see, the functions $\varphi^{\pm}(k)$ are analytic in the upper and lower half-planes of complex $k$, respectively.

After the Fourier transformation of Eq. (30), we obtain

$$\varphi^+(k) + \varphi^-(k) = g_0(k) + \chi(k)\, \varphi^+(k), \tag{A8}$$

where

$$\chi(k) = \Pi(k)\, g_0(k). \tag{A9}$$

From (A8) follows

$$\varphi^+(1 - \chi) = g_0 - \varphi^-. \tag{A10}$$

Then, we present $(\chi - 1)$ as

$$1 - \chi = \frac{\Gamma^+}{\Gamma^-}, \tag{A11}$$

where $\Gamma^{\pm}(k)$ are some analytic functions in the upper and lower half-planes of complex $k$, respectively. From (A8), we obtain

$$\Gamma^+ \varphi^+ = \Gamma^- V_0 - \Gamma^- \varphi^-. \tag{A12}$$

To solve this equation, we have to present $\Gamma^- g_0$ as a sum of functions being analytic in the upper and lower half-plane of complex $k$, respectively:

$$\Gamma^- g_0 = \Lambda^+ + \Lambda^-. \tag{A13}$$

After that, Eq. (A12) acquires the required form,

$$\Gamma^+ \varphi^+ - \Lambda^+ = \Lambda^- - \Gamma^- \varphi^-, \tag{A14}$$

with the functions analytical in upper half-plane on the left side, and the functions analytical in lower half-plane on the

right-hand side of this equation. Thus, the function on the left and the function on the right determine the same entire function $P(k)$, which can be taken as a polynom with the coefficients to satisfy the asymptotic behavior (31). Using Eq. (A14), we obtain

$$\varphi^+ = \frac{P + \Lambda^+}{\Gamma^+}, \tag{A15}$$

$$\varphi_- = \frac{\Lambda^- - P}{\Gamma^-}. \tag{A16}$$

Now we have to find $\Gamma^\pm$ and $\Lambda^\pm$.

Let us assume $\Pi(k) \simeq \Pi(0) = \text{const}$ (the usual assumption when we are looking for the screening length). The inverse screening length $\kappa$ in the bulk is related to $\Pi_0$ via $\kappa^2 = -4\pi e^2 \Pi$. The function $1 - \chi$ can be presented as

$$1 - \chi = 1 + \frac{\kappa^2}{k^2 + q^2} = \frac{(k + i\sqrt{\kappa^2 + q^2})(k - i\sqrt{\kappa^2 + q^2})}{(k + iq)(k - iq)}, \tag{A17}$$

which gives

$$\Gamma^+ = \frac{k + i\sqrt{\kappa^2 + q^2}}{k + iq}, \tag{A18}$$

$$\Gamma^- = \frac{k - iq}{k - i\sqrt{\kappa^2 + q^2}}. \tag{A19}$$

Note that with this choice of $\Gamma^\pm$, the function $1/\Gamma^-(k)$ is also an analytic function of $k$ in the lower half-plane of complex $k$.

The function (A13) can be presented as

$$\Gamma^- g_0 = \frac{k - iq}{k - i\sqrt{\kappa^2 + q^2}} \frac{4\pi e^2}{q^2 + k^2} = \frac{4i\pi e^2}{\sqrt{\kappa^2 + q^2} + q} \left( \frac{1}{k + iq} - \frac{1}{k - i\sqrt{\kappa^2 + q^2}} \right), \tag{A20}$$

which leads to

$$\Lambda_+ = \frac{4i\pi e^2}{\sqrt{\kappa^2 + q^2} + q} \frac{1}{k + iq}, \tag{A21}$$

$$\Lambda^- = -\frac{4i\pi e^2}{\sqrt{\kappa^2 + q^2} + q} \frac{1}{k - i\sqrt{\kappa^2 + q^2}}. \tag{A22}$$

Substituting (A18), (A19), (A21), and (A22) into (A15) and (A16), we obtain

$$\varphi^+ = \frac{P\sqrt{\kappa^2 + q^2}\,(k + iq) + 4i\pi e^2}{\sqrt{\kappa^2 + q^2}\,(k + i\sqrt{\kappa^2 + q^2})}, \tag{A23}$$

$$\varphi^- = -\frac{P\sqrt{\kappa^2 + q^2}\,(k - i\sqrt{\kappa^2 + q^2}) + 4i\pi e^2}{\sqrt{\kappa^2 + q^2}\,(k - iq)}. \tag{A24}$$

Using Eq. (A5), we get

$$W(k) = \frac{P\sqrt{\kappa^2 + q^2}\,(k + iq) + 4i\pi e^2}{\sqrt{\kappa^2 + q^2}\,(k + i\sqrt{\kappa^2 + q^2})} - \frac{P\sqrt{\kappa^2 + q^2}\,(k - i\sqrt{\kappa^2 + q^2}) + 4i\pi e^2}{\sqrt{\kappa^2 + q^2}\,(k - iq)} \tag{A25}$$

and

$$W(z) = \int \frac{dk}{2\pi} e^{ikz} \left[ \frac{P(k)\sqrt{\kappa^2 + q^2}\,(k + iq) + 4i\pi e^2}{\sqrt{\kappa^2 + q^2}\,(k + i\sqrt{\kappa^2 + q^2})} - \frac{P(k)\sqrt{\kappa^2 + q^2}\,(k - i\sqrt{\kappa^2 + q^2}) + 4i\pi e^2}{\sqrt{\kappa^2 + q^2}\,(k - iq)} \right]. \tag{A26}$$

Thus, for $z > 0$ we find

$$W(z) = e^{-qz} \frac{P(iq)\sqrt{\kappa^2 + q^2}\,(q - \sqrt{\kappa^2 + q^2}) + 4\pi e^2}{\sqrt{\kappa^2 + q^2}} = e^{-qz} \left[ \frac{4\pi e^2}{\sqrt{\kappa^2 + q^2}} - P(iq)\,(\sqrt{\kappa^2 + q^2} - q) \right], \tag{A27}$$

while for $z < 0$

$$W(z) = e^{z\sqrt{\kappa^2 + q^2}} \left[ \frac{4\pi e^2}{\sqrt{\kappa^2 + q^2}} - P(-i\sqrt{\kappa^2 + q^2}) \times (\sqrt{\kappa^2 + q^2} - q) \right]. \tag{A28}$$

If we take

$$P = \frac{2\pi e^2}{(\sqrt{\kappa^2 + q^2} - q)\sqrt{\kappa^2 + q^2}} \tag{A29}$$

as constant, which does not depend on $k$, then we finally obtain the formula (32).

## APPENDIX B: CALCULATION OF FUNCTION $g(r)$ IN THE CASE OF SCREENING BY BULK ELECTRONS

To determine the screening length, we have to calculate integral (34) for large $r$. After integrating over angle, we obtain

$$g(r) = \frac{e^2}{2\pi} \int_0^\infty \frac{q\,dq}{\sqrt{\kappa^2 + q^2}} \int_0^{2\pi} d\varphi\, e^{iqr\cos\varphi} = e^2 \int_0^\infty \frac{J_0(qr)\,q\,dq}{\sqrt{\kappa^2 + q^2}}. \tag{B1}$$

Integral (B1) can be calculated exactly [56],

$$g(r) = \frac{e^2}{r} \sqrt{\frac{\pi\kappa r}{2}} [I_{-1/2}(\kappa r) - \mathbf{L}_{-1/2}(\kappa r)], \tag{B2}$$

where $I_\nu(z)$ and $\mathbf{L}_\nu(z)$ are the modified Bessel and Struve functions, respectively.

For $z \gg 1$, one can use the asymptotics [57] $\mathbf{L}_{-1/2}(z) = I_{1/2}(z) + 0(z^{-3/2})$. Then, we get

$$g(r) \simeq \frac{e^2}{r} \sqrt{\frac{\pi\kappa r}{2}} [I_{-1/2}(\kappa r) - I_{1/2}(\kappa r)]. \tag{B3}$$

These modified Bessel functions can be presented by elementary functions [57]

$$I_{-1/2}(z) = \sqrt{\frac{2z}{\pi}} \frac{\cosh z}{z}, \quad I_{1/2}(z) = \sqrt{\frac{2z}{\pi}} \frac{\sinh z}{z}. \tag{B4}$$

Substituting (B4) to (B3), we obtain

$$g(r) = \frac{e^2\, e^{-\kappa r}}{r}, \qquad \kappa r \gg 1. \tag{B5}$$

Thus, the behavior of function $g(r)$ at large distances corresponds to the screened Coulomb interaction determined by the screening length $\kappa^{-1}$.


[1] M. Z. Hasan and C. L. Kane, Colloquium: Topological insulators, Rev. Mod. Phys. **82**, 3045 (2010).

[2] X.-L. Qi and S.-C. Zhang, Topological insulators and superconductors, Rev. Mod. Phys. **83**, 1057 (2011).

[3] H. H. Kung, S. Maiti, X. Wang, S.-W. Cheong, D. L. Maslov, and G. Blumberg, Chiral Spin Mode on the Surface of a Topological Insulator, Phys. Rev. Lett. **119**, 136802 (2017).

[4] X. Dai, Z. Z. Du, and H. Z. Lu, Negative Magnetoresistance Without Chiral Anomaly in Topological Insulators, Phys. Rev. Lett. **119**, 166601 (2017).

[5] A. Agarwala and V. B. Shenoy, Topological Insulators in Amorphous Systems, Phys. Rev. Lett. **118**, 236402 (2017).

[6] A. Pertsova and C. M. Canali and A. H. MacDonald, Quantum Hall edge states in topological insulator nanoribbons, Phys. Rev. B **94**, 121409(R) (2016).

[7] A. Mook, J. Henk, and I. Mertig, Spin dynamics simulations of topological magnon insulators: From transverse current correlation functions to the family of magnon Hall effects, Phys. Rev. B **94**, 174444 (2016).

[8] B. Li and A. A. Kovalev, Chiral topological insulator of magnons, Phys. Rev. B **97**, 174413 (2018).

[9] A. Dankert, P. Bhaskar, D. Khokhriakov, I. H. Rodrigues, B. Karpiak, M. V. Kamalakar, S. Charpentier, I. Garate, and S. P. Dash, Origin and evolution of surface spin current in topological insulators, Phys. Rev. B **97**, 125414 (2018).

[10] Y. Araki and K. Nomura, Skyrmion-induced anomalous Hall conductivity on topological insulator surfaces, Phys. Rev. B **96**, 165303 (2017).

[11] M. Schmitt and P. Wang, Universal nonanalytic behavior of the nonequilibrium Hall conductance in Floquet topological insulators, Phys. Rev. B **96**, 054306 (2017).

[12] M. Schüler and P. Werner, Tracing the nonequilibrium topological state of Chern insulators, Phys. Rev. B **96**, 155122 (2017).

[13] K. Nakata, S. K. Kim, J. Klinovaja, and D. Loss, Magnonic topological insulators in antiferromagnets, Phys. Rev. B **96**, 224414 (2017).

[14] T. K. Bhowmick, A. De, and R. K. Lake, High figure of merit magneto-optics from interfacial skyrmions on topological insulators, Phys. Rev. B **98**, 024424 (2018).

[15] Y. Xie, Y. Tan, and A. W. Ghosh, Spintronic signatures of Klein tunneling in topological insulators, Phys. Rev. B **96**, 205151 (2017).

[16] P. B. Ndiaye, C. A. Akosa, M. H. Fischer, A. Vaezi, E. A. Kim, and A. Manchon, Dirac spin-orbit torques and charge pumping at the surface of topological insulators, Phys. Rev. B **96**, 014408 (2017).

[17] S. Ghosh and A. Manchon, Spin-orbit torque in two-dimensional antiferromagnetic topological insulators, Phys. Rev. B **95**, 035422 (2017).

[18] E. Locane and P. W. Brouwer, Current-induced switching of magnetic molecules on topological insulator surfaces, Phys. Rev. B **95**, 125437 (2017).

[19] S. Zhang and A. Fert, Conversion between spin and charge currents with topological insulators, Phys. Rev. B **94**, 184423 (2016).

[20] N. Okuma, M. R. Masir, and A. H. MacDonald, Theory of the spin-Seebeck effect at a topological-insulator/ferromagnetic-insulator interface, Phys. Rev. B **95**, 165418 (2017).

[21] R. Dey, N. Prasad, L. F. Register, and S. K. Banerjee, Conversion of spin current into charge current in a topological insulator: Role of the interface, Phys. Rev. B **97**, 174406 (2018).

[22] L. Chotorlishvili, A. Ernst, V. K. Dugaev, A. Komnik, M. G. Vergniory, E. V. Chulkov, and J. Berakdar, Magnetic fluctuations in topological insulators with ordered magnetic adatoms: Cr on Bi2Se3 from first principles, Phys. Rev. B **89**, 075103 (2014).

[23] D. Nandi, I. Sodemann, K. Shain, G. H. Lee, K. F. Huang, C. Z. Chang, Y. Ou, S. P. Lee, J. Ward, J. S. Moodera, P. Kim, and A. Yacoby, Logarithmic singularities and quantum oscillations in magnetically doped topological insulators, Phys. Rev. B **97**, 085151 (2018).

[24] A. Vezvaee, A. Russo, S. E. Economou, and E. Barnes, Topological insulator ring with magnetic impurities, Phys. Rev. B **98**, 035301 (2018).

[25] S. Stagraczyński, L. Chotorlishvili, V. K. Dugaev, C. L. Jia, A. Ernst, A. Komnik, and J. Berakdar, Topological insulator in a helicoidal magnetization field, Phys. Rev. B **94**, 174436 (2016).

[26] A. Amaricci, J. C. Budich, M. Capone, B. Trauzettel, and S. Sangiovammi, Strong correlation effects on the topological quantum phase transitions in three dimensions, Phys. Rev. B **93**, 235112 (2016).

[27] A. Amaricci, L. Privitera, F. Petocchi, M. Capone, G. Sangiovanni, and B. Trauzettel, Edge state reconstruction from strong correlations in quantum spin insulators, Phys. Rev. B **95**, 205120 (2017).

[28] A. Amaricci, A. Valli, G. Sangiovanni, B. Trauzettel, and M. Capone, Coexistence of metallic edge states and antiferromagnetic ordering in correlated topological insulators, Phys. Rev. B **98**, 045133 (2018).

[29] Y. Seo, G. Song, and S. J. Sin, Strong correlation effects on surface of topological insulators via holography, Phys. Rev. B **96**, 041104(R) (2017).

[30] S. Han and E.-G. Moon, Long-range Coulomb interaction effects on the topological phase transitions between semimetals and insulators, Phys. Rev. B **97**, 241101(R) (2018).

[31] A. Matsugatani, Y. Ishiguro, K. Shiozaki, and H. Watanabe, Universal Relation Among the Many-Body Chern Number, Rotation Symmetry, and Filling, Phys. Rev. Lett. **120**, 096601 (2018).

[32] J. Gonzáles, F. Guinea, and M. A. H. Vozmediano, Marginal-Fermi-liquid behavior from two-dimensional Coulomb interaction, Phys. Rev. B **59**, R2474 (1999).

[33] J. Gonzáles, F. Guinea, and M. A. H. Vozmediano, Electron-electron interaction in graphene sheets, Phys. Rev. B **63**, 134421 (2001).

[34] M. S. Foster and I. L. Aleiner, Graphene via large $N$: A renormalization group study, Phys. Rev. B **77**, 195413 (2008).
[35] M. Z. Hasan and J. E. Moore, Three-dimensional topological insulators, Annu. Rev. Condens. Matter Phys. **2**, 55 (2011).
[36] H.-K. Tang, J. N. Leaw, J. N. B. Rodrigues, I. F. Herbut, P. Sengupta, F. F. Assaad, and S. Adam, The role of electron-electron interactions in two-dimensional Dirac fermions, Science **361**, 570 (2018).
[37] W. C. Yu, Y. C. Li, P. D. Sacramento, and H. Q. Lin, Reduced density matrix and order parameters of a topological insulator, Phys. Rev. B **94**, 245123 (2016).
[38] J. Manousakis, A. Altland, D. Bagrets, R. Egger, and Y. Ando, Majorana qubits in a topological insulator nanoribbon architecture, Phys. Rev. B **95**, 165424 (2017).
[39] B. Monserrat and D. Vanderbilt, Temperature Effects in the Band Structure of Topological Insulators, Phys. Rev. Lett. **117**, 226801 (2016).
[40] Y. Yao, M. Sato, T. Nakamura, N. Furukawa, and M. Oshikawa, Theory of electron spin resonance in one-dimensional topological insulators with spin-orbit couplings: Detection of edge states, Phys. Rev. B **96**, 205424 (2017).
[41] Y. Hama and N. Nagaosa, Electromagnon on the surface of a magnetic topological insulator, Phys. Rev. B **98**, 045423 (2018).
[42] L. Hedin, New method for calculating the one-particle Green-Fus functions-A with application to the electron-gas problem, Phys. Rev. **139**, A796 (1965).
[43] I. Aguilera, C. Friedrich, G. Bihlmayer, and S. Blügel, GW study of topological insulators $Bi_2Se_3$, $Bi_2Te_3$, and $Sb_2Te_3$: Beyond the perturbative one-shot approach, Phys. Rev. B **88**, 045206 (2013).
[44] T. Förster, P. Krüger, and M. Rohlfing, GW calculations for $Bi_2Te_3$ and $Sb_2Te_3$ thin films: Electronic and topological properties, Phys. Rev. B **93**, 205442 (2016).
[45] I. A. Nechaev and E. V. Chulkov, Effects of the electron-electron interaction on the surface of three-dimensional topological insulators, JETP Lett. **96**, 480-485 (2012).
[46] C. L. Kane and E. J. Mele, Quantum Spin Hall Effect in Graphene, Phys. Rev. Lett. **95**, 226801 (2005).
[47] D. C. Elias, R. V. Gorbachev, A. S. Mayorov, S. V. Morozov, A. A. Zhukov, P. Blake, L. A. Ponomarenko, I. V. Grigorieva, K. S. Novoselov, F. Guinea, and A. K. Geim, Dirac cones reshaped by interaction effects in suspended graphene, Nat. Phys. **7**, 701 (2011).
[48] M. I. Katsnelson, *Graphene: Carbon in Two Dimensions* (Cambridge University Press, Cambridge, UK, 2012).
[49] L. Fu and C. L. Kane, Topological insulators with inversion symmetry, Phys. Rev. B **76**, 045302 (2007).
[50] M. Ezawa, Magnetic second-order topological insulators and semimetals, Phys. Rev. B **97**, 155305 (2018).
[51] H. Ishida, A. Liebsch, and D. Wortmann, Topological invariants of band insulators derived from the local-orbital based embedding potential, Phys. Rev. B **96**, 125413 (2017).
[52] H. Araki, T. Fukui, and Y. Hatsugai, Entanglement Chern number for three-dimensional topological insulators: Characterization by Weyl points of entanglement Hamiltonians, Phys. Rev. B **96**, 165139 (2017).
[53] L. A. Wray, S.-Y. Xu, Y. Xia, D. Hsieh, A. V. Fedorov, Y. S. Hor, R. J. Cava, A. Bansil, H. Lin and M. Z. Hasan, A topological insulator surface under strong Coulomb, magnetic, and disorder perturbations, Nat. Phys. **7**, 32 (2011).
[54] P. M. Morse and H. Feshbach, *Methods of Theoretical Physics* (McGraw-Hill, New York, 1953), Vol. 1, Chap. 8.
[55] J. Mathews and R. L. Walker, *Mathematical Methods in Physics* (Addison-Wesley, New York, 1970).
[56] A. P. Prudnikov, Y. A. Brychkov, and O. I. Marichev, *Integrals and Series* (Gordon and Breach, New York, 1986), Vol. 2, p. 179.
[57] *Handbook of Mathematical Functions*, edited by M. Abramowitz and I. I. Stegun, National Bureau of Standards Applied Mathematics Series 55 (National Bureau of Standards, Washington, DC, 1964), p. 498.